

# Skillful Operation of Working Plate for Grasp Less Ball Handling with an Industrial Dual-Arm Robot Considering Temperature of Joint Motors

Takumi Soga\*, Hiroaki Hanai, Toshiki Hirogaki, and Eiichi Aoyama

Department of Mechanical Engineering, Doshisha University, Kyoto, Japan

Email: 0ve5f61638f1z6t@ezweb.ne.jp (T.S.); cyjh1501@mail4.doshisha.ac.jp (H.H.); thirogak@mail.doshisha.ac.jp (T.H.); eaoyama@mail.doshisha.ac.jp (E.A.)

\*Corresponding author

Manuscript received April 10, 2023; revised May 10, 2023; accepted May 24, 2023; published October 23, 2024

**Abstract**—This paper discusses a method of skillful plate manipulation that considers the temperature of the joint motors in a work plate manipulation operation using an industrial dual-arm robot. First, we focused on the temperature of the joint motors of the robot after prolonged operation in work plate manipulation. Due to rise in joint motor temperature, a positive correlation was observed between the thermal displacement between joints and the plate angle error. We confirmed the assumption that the temperature rise of the joint motors causes the motion error of the robot. Additionally, we found that the motion error in the plate manipulation motion can be improved by correcting the generated angle error.

**Keywords**—industrial dual-arm robot, temperature of joint motors, grasp less ball handling, motion errors, ball rolling, circular motion

## I. INTRODUCTION

In recent years, the industrial usefulness of dual-arm robots has been demonstrated in applications such as grasping and changing thin [1], flexible metal sheets and flexible wrapping cloths (furoshiki) [2]. These are applications based on the grasping motion. However, when we consider a case in which a human manipulates an object in the workplace, not all actions are necessarily performed by grasping the object. In many cases, an object is brought into contact with the environment and manipulated (pushed or rolled) using gravity or frictional force, allowing work to be performed with a small load. An example is grasping less manipulation [3]. In a previous study [4], we examined the case in which a sphere rolls in a circular path with grasp less handling on the plane plate of a dual-arm robot and showed that it is possible to diagnose the dynamic motion accuracy of the two-axis turning motion of the plate from the radial error of the rolling circular motion. And, in a dual-armed robot, a closed-link state was created by grasping the plate with both arms to ensure a certain degree of support rigidity. This enabled a working range similar to that of human motion, and was shown to be practical [5]. In addition, in recent years, as factory automation has progressed, industrial robots have been widely introduced, and robots with more precise motion are required. However, motion errors due to continuous prolonged operation of industrial robots are a problem for which no clear cause or remedy has been established. In this study, we focused on the temperature of the joint motors of a robot during long-term operation and examined the effect of joint temperature on the rolling circular motion of a ball by plate manipulation, so that the robot can be automated for a

long time while maintaining high motion performance. Power consumption changes due to temperature changes in the joint motors, thermal displacement between joints, and angular changes in the plates are measured, and compensation of the motion errors generated is also discussed.

## II. EXPERIMENTAL MODEL

### A. Industrial Dual-Arm Robot

This study used MOTOMAN-DIA10, a dual-arm robot manufactured by Yaskawa Electric Corporation, as shown in Fig. 1. It was developed based on the human upper body and is of the same size as an adult male. The left arm is the master arm (Arm L), and the right arm is the slave arm (Arm R). The model of the joints (S to T) and the distance between the links of the dual-arm robot are shown in Fig. 2. Each arm has seven joints and can move in a manner similar to that of the human arm. In addition, the robot is equipped with one joint to rotate the torso for 15 degrees of freedom. Each arm can hold a weight of 98 N (10 kgf); and both arms can hold 196 N (20 kgf). The plate used in the experiment was made of acrylic and measured 600 mm × 450 mm × 20 mm, with a flatness of ±0.003 mm. The plate was supported by flat jaws and clamped from above and below. The coordinate system shown in Fig. 1 was set up, and the work plate was manipulated by grasping it with both arms and swiveling it around its  $X_p$  and  $Y_p$  axes.

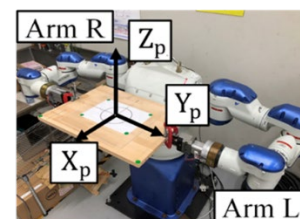


Fig. 1. Dual-arm robot.

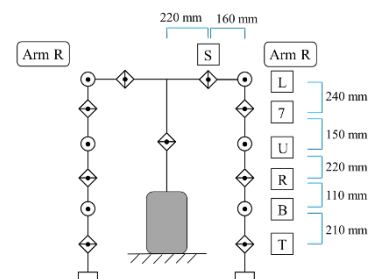


Fig. 2. Composition.

### B. Coordinate Systems and Basic Theory

As a method for diagnosing the accuracy of motion of two straight axes, the DBB method [6], which gives a circular motion command and focuses on the motion error, is a well-known method. In this case, assuming that the angular velocity of the center of a circular motion of radius  $R$  is  $\omega$ , time is  $t$ , and the initial phase is zero, the position commands for the two orthogonal straight axes ( $X_P$  and  $Y_P$  axes) are given as the sine function  $R\sin\omega t$  for the  $X_P$  axis and the cosine function  $R\cos\omega t$ , or  $R\sin(\omega t+90^\circ)$  for the  $Y_P$  axis to diagnose motion error. In this study, the motion of the ball on the plate was based on the airplane dynamics coordinate system,  $O_P - X_P Y_P Z_P$ , as shown in Fig. 3 [7]. The  $X_P$  and  $Y_P$  axis rotations are defined as the pitch and roll, respectively.

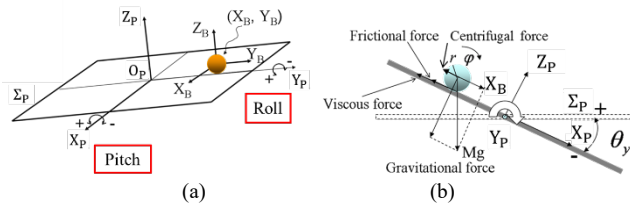


Fig. 3. Model of the ball rolling on the work plate, (a) Three-dimensional coordinate, (b) Sectional view in two-dimensional coordinate.

Let  $\Sigma_P$  be a coordinate system fixed to the plate, be a coordinate system fixed to the position of the center of gravity of the object (the axis is orthogonal to the contact surface with the plate), and  ${}^P X_B$  and  ${}^P Y_B$  be the  $\Sigma_B$  positions viewed from  $\Sigma_P$ . The radius  $r$  (mm), central rotation angle  $\varphi$  (rad), mass  $M$  (kg), and, for simplicity, the damping coefficient  $D$ , which is proportional to the velocity of the center of gravity of the ball, satisfy the following relation:  $D_M = 5D/7M$ . The equation of motion for the center of gravity of the ball is expressed as Eq. (1). The input equation for a circular orbit is given by Eq. (2).

$$\begin{bmatrix} \frac{d^{2P} X_B}{dt^2} \\ \frac{d^{2P} Y_B}{dt^2} \end{bmatrix} = \frac{5}{7}g \begin{bmatrix} \theta_y \\ \theta_x \end{bmatrix} - D_M \begin{bmatrix} \frac{d^P X_B}{dt} \\ \frac{d^P Y_B}{dt} \end{bmatrix} - \frac{5}{7} \begin{bmatrix} {}^P X_B \left( \frac{d\theta_y}{dt} \right)^2 \\ {}^P Y_B \left( \frac{d\theta_x}{dt} \right)^2 \end{bmatrix} \quad (1)$$

$$\begin{cases} \theta_y(t) = \theta_{y0} \sin(\omega_1 t + \pi/2) \\ \theta_x(t) = \theta_{x0} \sin(\omega_2 t) \end{cases} \quad (2)$$

In Eq. (1), the plate tilt angle  $\theta$  is a function of time,  $\theta_0$  is the maximum tilt angle,  $\theta_y$  and  $\theta_x$  are the input angles around the  $Y_P$  and  $X_P$  axes, respectively. The input equation for a circular orbit consists of a combination of  $X_P$  and  $Y_P$  axis rotations. Here, we discuss the input equation for a circular orbit when  $\theta_{y0} = \theta_{x0} = 3^\circ$  and  $\omega_1 = \omega_2 = 2.4$  rad/s.

## III. EXPERIMENTAL METHOD

### A. Teaching Methods for Robot

The teaching point angles for the circular orbit manipulation of the ball by the dual-armed robot are the four points at which one cycle of the input equation (Eq. (2)) is divided into four equal parts. Fig. 4 shows the teaching points and numbers. The teaching points are  $T_1(\theta_{x0}, 0)$ ,  $T_2(0, \theta_{y0})$ ,  $T_3(-\theta_{x0}, 0)$ , and  $T_4(0, -\theta_{y0})$ . Fig. 5 shows a Bode diagram

of the M22 mouse ball under the experimental conditions described in this study, which is a transfer function between the ball rolling radius  $R$  mm as output and the plate tilt angle  $\theta$  rad as input. The response of the ball is delayed by  $170^\circ$  relative to the input slope. Thus, the ball rolled up the slope of the plate. Fig. 6 shows a model of a dual-arm robot grasping a plate. Teaching was performed by placing a gyro sensor at the center of the plate such that the tilt angle was the target angle. Teaching consists of a posture taken by the  $X_P$  and  $Y_P$  axes turning commands as XYZ Cartesian coordinates, and the speed command indicates the turning speed of the joints. The accuracy of the repetitive positioning of the robot is  $\pm 0.1$  mm, in accordance with JIS B8432. The maximum speed of each joint is listed in Table 1. The closer it is to the end effector of the arm, the lower the reduction ratio, the higher the maximum speed, and the lower the allowable torque become (see Table 1).

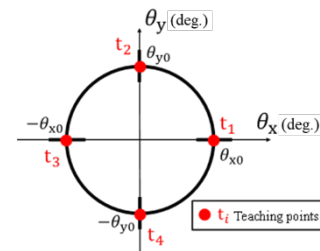


Fig. 4. Teaching points of circular orbit.

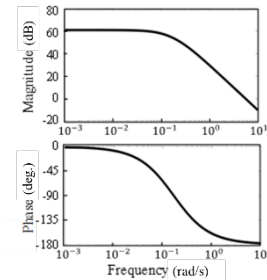


Fig. 5. Bode diagram.

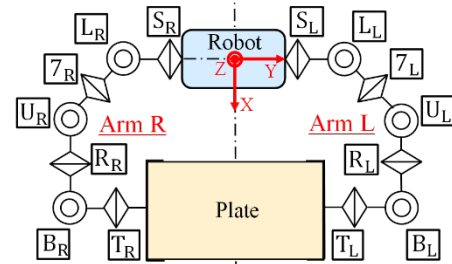


Fig. 6. Robot model.

Table 1. Elongation at each section

Joint	Maximum angular velocity (rad/s)	Maximum angular velocity (deg./s)
S	2.97	170
L	2.97	170
7	2.97	170
U	2.97	170
R	4.36	250
B	4.36	250
T	8.73	500

### B. Measurement Method

The trajectory of the ball on the plate was measured by placing a gyro sensor at the center of the plate and measuring the taught turning angle and the turning angle during movement. The trajectory was analyzed using an analysis

program that recorded a movie 300 mm above the plate. The program used four markers placed on the plate as coordinate references and calculated the coordinates based on the position of the ball in relation to the markers. The motion of the ball on the plate plane is treated as the planar motion of the ball.

### C. Determination of Joints to Measure Temperature Change and Power Consumption Change

Fig. 7 shows the amplitude of the rotation angle of each joint when outputting a circular trajectory.

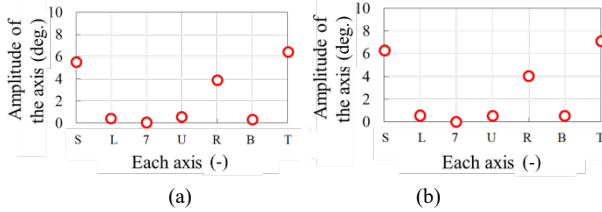


Fig. 7. Amplitude of the rotation angle for each axis bode diagram, (a) left arm, (b) right arm.

This figure shows that only joints  $s$ ,  $r$ , and  $t$  act when outputting a circular trajectory; therefore, we focused on these three joints in this study.

### D. Measurement of Temperature Change and Power Consumption of Each Joint

To measure the temperature change at each joint, a paste-type thermocouple for surface measurement (mf-o-k) manufactured by toa electric appliances was used. A marpossgemtmutp instantaneous power monitor was used to measure changes in power consumption at each joint. The sampling period of the output was 3 ms, and the measured value of the power signal was converted into a dimensionless percentage after processing the sensor data. This device measures the current and voltage between the servo amplifier and servo motor and calculates the power. This measurement device was connected in parallel with six channels, enabling simultaneous power measurement of the six axes.

## IV. RESULTS AND CONSIDERATION

### A. Circular Orbit Change under Load and Long Continuous Operation

Fig. 8 shows the circular trajectory of the ball at the beginning and after 4 h of operation with no load and with a load of 1 kg on each of the four corners of the plate for a total of 4 kg, with the robot grasping the plate, as shown in Fig. 1.

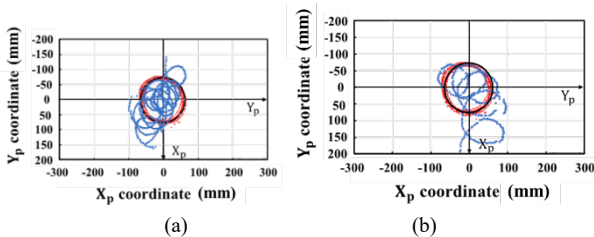


Fig. 8. Circular orbit after 4 h, (a) Without load, (b) With 4 kg load.

Fig. 8 shows that regardless of whether the plate was loaded or unloaded, the circular trajectory of the ball, showed a deviation after 4 h. With the load, the deviation of the trajectory and center of the ball was larger than that without

the load, and the trajectory mainly deviated in the positive direction of the  $X_p$  axis.

### B. Change in Joint Temperature and Power Consumption During Long Continuous Operation

Figs. 9 and 10 show the temperature and power consumption of the shoulder ( $S$ ), elbow ( $R$ ), and wrist ( $T$ ) joints with and without a load (4 kg).

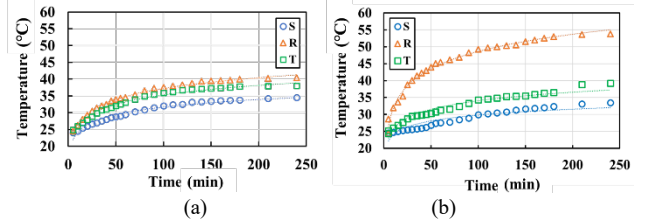


Fig. 9. Temperature change for 4 h, (a) Without load, (b) With 4 kg load.

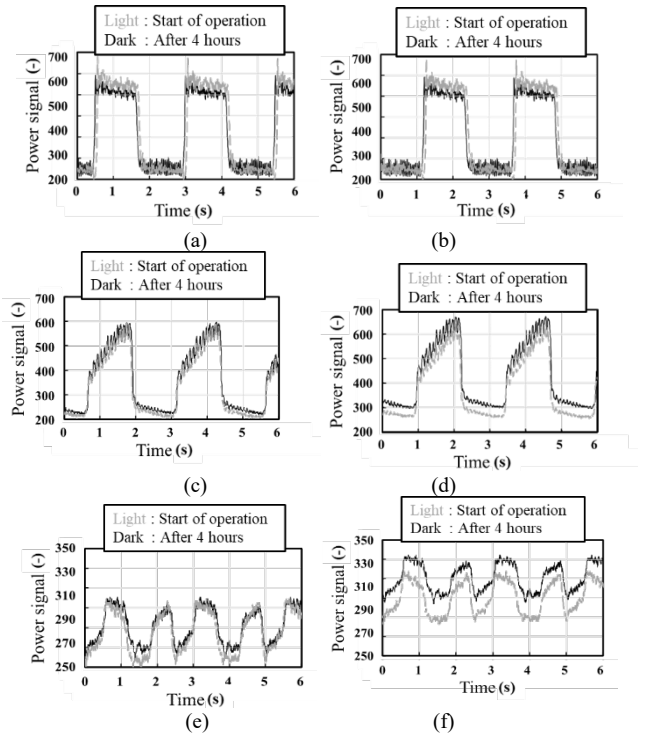


Fig. 10. Change in power consumption, (a) S joint (without load), (b) S joint (with 4 kg load), (c) R joint (without load), (d) R joint (with 4 kg load), (e) T joint (without load), (f) T joint (with 4 kg load).

Fig. 9 shows that the temperature of each joint of the robot tends to increase during long-term continuous operation, regardless of whether the robot is loaded or unloaded. In particular, the temperature rise in the  $R$ -joint with a load was particularly pronounced. Fig. 10 shows that the average power consumption of the  $R$  and  $T$  joints increased by more than 10% during long-term operation with a load compared with the case without a load. Based on these results, the rolling circular motion of the ball in the plate 2-axis turning motion control in this experiment places a large load on the  $R$  joint.

### C. Arm Extension and Plate Angle Change in Thermal Displacement

Using the results in Fig. 9 and the coefficient of linear expansion of the arm, we calculated the theoretical elongation between each link as the temperature increased and used the DH method in robot sequential kinematics to calculate the theoretical elongation of the plate in the  $X_p$  and  $Y_p$  axes.

Actual arm extension was measured using a laser displacement meter, and the results are listed in Table 2. A schematic of this process is shown in Fig. 11.

Table 2. Elongation at each section

Section	Predicted Elongation (mm)	Measured Elongation (mm)
1	0.0423	0.0054
2	0.1382	0.0994
3	0.2168	0.1221
4	0.0885	0.0623
$X_p$ direction	0.2731	0.1641
$Y_p$ direction	0.0451	0.0021

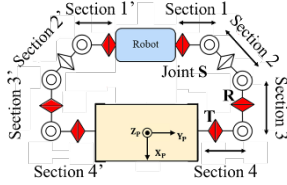


Fig. 11. Section for elongation.

Table 2 shows that the elongation (thermal displacement) of Sections II and III in Fig. 11 is remarkable, and that the displacement is mainly in the  $X_p$  axis direction in the position coordinate of the plate. Because the displacement in the  $Y_p$  axis direction is less than 1/10 of that in the  $X_p$  axis direction, the former is ignored. Table 3 lists the plate angle changes at the start of the operation and after 4 h.

Table 3. Pitch and roll change with temperature change

	Start of operation	4 h later	$\Delta\theta$
Max pitch (deg.)	2.168	2.183	0.015
Min pitch (deg.)	-2.402	-2.385	0.017
Max roll (deg.)	3.031	3.174	0.143
Min roll (deg.)	-2.411	-2.215	0.196

Table 3 shows that the angular error of the roll is 10 times larger than that of the pitch after 4 h of operation. In particular, the maximum and minimum values of roll tended to increase, which can be predicted to cause a deviation in the trajectory of the ball in the positive direction of the  $X_p$  axis of the plate. The angular change in the output to the plate is considered to be related to the temperature increase and thermal displacement of the joint. As a representative example, Fig. 12 shows the maximum and minimum changes in the roll for the thermal displacement between U and B in Fig. 11. The thermal displacement between U and B is denoted as  $\Delta L$ .

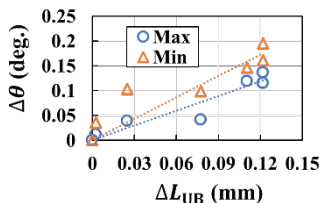


Fig. 12. Angular error in thermal displacement.

Fig. 12 shows that the angular error between the maximum and minimum values of the roll tends to increase as the thermal displacement  $\Delta L$  between U and B increases. This implies that as the thermal displacement  $\Delta L$  between U and B increases, the roll, which is the ratio of positive rotation in the  $Y_p$  axis rotation, increases, as shown in Fig. 12, where the circular trajectory of the ball deviates in the positive direction

of the  $X_p$  axis. The cause of the increase in the positive rotation ratio in the  $Y_p$  axis direction may be that the thermal displacement of the joint caused a deflection in the negative direction of the  $Z_p$  axis, causing the plate to tilt in the positive direction of the  $Y_p$  axis. In addition to the thermal displacement of the joints, there may be other causes, such as the joint motors being affected by heat and being unable to correctly represent the commanded angle. Therefore, thermal compensation, which focuses on the temperature, is promising for maintaining high-precision motion.

#### D. Correction of Ball Trajectory by Angle Compensation

Assuming that the  $Y_p$  axis turning angle of the plate immediately after the start of motion is  $\theta_0$ , the  $Y_p$  axis turning angle of the plate after the temperature rise is  $\theta_a$ , and the amount of angle change is  $\Delta\theta(\Delta t)$ , the  $Y_p$  axis turning angle of the plate after temperature rise  $\theta_a$  is presented in Eq. (3). In correcting the angle of the plate, the angle is corrected to the original angle by decreasing the amount of angle change  $\Delta\theta(\Delta t)$  that has occurred.

$$\theta_a = \theta_0 + \Delta\theta(\Delta t) \quad (3)$$

The teaching angles are corrected around the  $Y_p$  axis, namely at teaching points  $t_2$  and  $t_4$  in Fig. 4, where the angle of roll is determined. The angle to be corrected was reduced by 0.14 at teaching point  $t_2$  and 0.19° at  $t_4$  from Table 4. Because the amount of change in pitch is approximately 1/10 the amount of change in roll, the former is ignored in Table 3. The trajectories of the ball before and after correction are shown in Fig. 13. As the angular velocity of the plate in this experiment was input at 2.4 rad/s, the theoretical period of the ball on the plate was 2.6 s. The period of the ball on the plate is defined as the period of its existence. If one period of the ball is 2.6 s and the period of the ball on the plate is defined as the existence period, the existence periods before and after the correction are listed in Table 4.

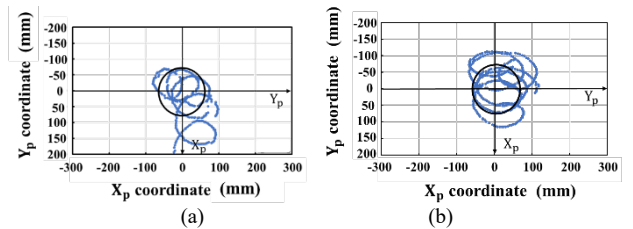


Fig. 13. Ball trajectory before and after correction.

Table 4. Period of existence before and after correction

	Before correction	After correction
Period of existence	3.3	6.3

## V. CONCLUSION

In this study, we focused on a method of skillful plate manipulation that considers the temperature of joint motors in a work-plate manipulation operation using an industrial dual-arm robot. In recent years, industrial robots have been forced to operate continuously for a long time, and we investigated the temperature change and power consumption of a joint motor during a continuous and prolonged work plate manipulation operation using an industrial dual-arm robot. The following conclusions were drawn.



- 1) The increase in the joint temperature owing to the long continuous operation causes thermal displacement and angular error, resulting in errors in the circular trajectory of the ball.
- 2) Thermal displacement and plate angular error tend to be positively correlated.
- 3) By correcting for the angular error, the circular trajectory of the ball and the period during which the ball was present on the plate could be improved.

#### CONFLICT OF INTEREST

The authors declare no conflict of interest.

#### AUTHOR CONTRIBUTIONS

Takumi Soga and Hiroaki Hanai conducted the research, analyzed the data; Takumi Soga, Toshiki Hirogaki and Eiichi Aoyama wrote the paper; Hiroaki Hanai assisted with the writing; all authors had approved the final version.

#### ACKNOWLEDGMENT

We gratefully acknowledge the work of past and present members of our laboratory.

#### REFERENCES

- [1] S. Aoyama, T. Ueki, and T. Koshiba, "Regrasp motion planning for sheet metal bending by a dual-arm robot," *Japan Society for Precision Engineering*, vol. 78, no. 6, pp. 511–516, 2012.
- [2] H. Terada and K. Yagata, "Motion planning approach of a multi-robot system for furoshiki wrapping operation," *Japan Society for Precision Engineering*, vol. 76, no. 5, pp. 546–551, 2010.
- [3] Y. Aiyama, M. Inaba, and H. Inoue, "Pivoting: A new method of grasp less manipulation of object by robot fingers," in *Proc. 1993 IEEE/RSJ International Conference on Intelligent Robots and Systems (IROS '93)*, Yokohama, Japan, 1993, pp. 136–143.
- [4] W. Wu, T. Hirogaki, and E. Aoyama, "Investigation and improving method of two axes synchronous accuracy of plate pivot control with a dual arm robot by estimating ball rolling motion on the plate," *Transactions of the Japan Society of Mechanical Engineers*, vol. 78, no. 785, pp. 292–304, 2012.
- [5] W. Wu, T. Hirogaki, and E. Aoyama, "Motion control of rolling ball by operating the working plate with a dual-arm robot," *International Journal of Automation Technology*, vol. 6, no. 1, pp. 75–83, 2012.
- [6] Y. Kakino, Y. Ihara, A. Kamei, and T. Ise, "Study on the motion accuracy of NC machine tools (1st report) the measurement and evaluation of motion errors by double ball bar test," *Journal of the Japan Society for Precision Engineering*, vol. 52, no. 7, pp. 1193–1198, 1986.
- [7] M. Higashimori, K. Utsumi, Y. Omoto, and M. Kaneko, "Dynamic manipulation inspired by handling mechanism of pizza master," *Transactions of the Japan Society of Mechanical Engineers*, vol. 74, no. 743, pp. 1825–1833, 2008.

Copyright © 2024 by the authors. This is an open access article distributed under the Creative Commons Attribution License which permits unrestricted use, distribution, and reproduction in any medium, provided the original work is properly cited ([CC BY 4.0](https://creativecommons.org/licenses/by/4.0/)).